

VINILA MUNDAKKAL
LAKSHMANAN^{1,2}
APARNA KALLINGAL¹
SREEPRIYA SREEKUMAR^{1,2}

¹Department of Chemical
Engineering, National Institute of
Technology Calicut, Kozhikode,
Kerala, India

²Department of Robotics and
Automation, Adi Shankara
Institute of Engineering and
Technology, Kalady, India

SCIENTIFIC PAPER

UDC 547:544:519.6

INTERNAL MODEL CONTROL OF CUMENE PROCESS USING ANALYTICAL RULES AND EVOLUTIONARY COMPUTATION

Article Highlights

- Classical controllers have been implemented for the cumene process with much uncertainty
- IMC controller is designed for cumene production and is compared with the ZN tuning controller
- It is identified that the PI controller is apt for this specific cumene production process
- PSO-PI controller is designed to analyze performance with evolutionary computation techniques

Abstract

Cumene is a precursor for producing many organic chemicals and is thinner in paints and lacquers. Its production process involves one of the large-scale manufacturing processes with complex kinetics. Different classical control strategies have been implemented and compared in this process for the cumene reactor. As a system with large degrees of freedom, a novel approach for extracting the state space model from the COMSOL Multiphysics implementation of the system is adopted here. Internal Model Control (IMC) based PI and PID controllers are derived for the system. The system is reduced to the FOPDT and SOPDT model structure to derive the controller setting using Skogestad half rules. The integral time is modified for excellent set point tracking and faster disturbance rejection. From the analysis, it can be stated that the PI controller suits more for this specific process. The particle swarm optimization (PSO) algorithm, an evolutionary computation technique, is also used to tune the PI settings. The PI controllers with IMC, Zeigler Nichols, and PSO tuning are compared, and it can be concluded that the PSO PI controller settles at 45 s without any oscillations and settles down faster for the disturbance of magnitude 0.5 applied at $t = 800$ s. However, it is computationally intensive compared to other controller strategies.

Keywords: IMC PI, IMC PID, Skogestad half rule, Zeigler Nichols, PSO PI.

PID (Proportional-Integral-Derivative) controller is the widely adopted control strategy in the industry due to its simplicity in design and robustness. Besides, it

can be employed in many processes with wide operating conditions. Even though the PID controller owns only three design parameters, finding suitable values (settings) for them without a systematic method is difficult. A visit to a process industry will reveal a high count of poorly tuned PID controllers. The scope of the systematic approach for developing classical controllers with different tuning mechanisms to the cumene reactor in the cumene plant in HOCL, Kochi, is analyzed in this study.

Sigurd Skogestad has introduced analytic rules for reducing the model and tuning the PID controller [1]. Previous work in this area includes Ziegler and

Correspondence: A. Kallingal, Department of Chemical Engineering, National Institute of Technology Calicut, Kozhikode, Kerala, 673601, India.

E-mail: aparnak@nitc.ac.in

Paper received: 11 July, 2022

Paper revised: 23 March, 2023

Paper accepted: 22 June, 2023

<https://doi.org/10.2298/CICEQ220711014M>

Nichol's [2]. classic study and discussion on IMC PID-tuning mechanism by Rivera *et al.* [3]. For integrating processes, the Ziegler-Nichols settings produce good disturbance rejection, but in the case of processes with dominant delay, they produce quite poor performance and aggressive settings [4–6]. On the other hand, the analytically derived IMC settings by Rivera *et al.* [3] have a weak disturbance rejection for integrating processes [6–7]. Still, they are robust and have excellent setpoint change responses. In a multidimensional space, a great number of particles move around in the PID controller with a basic PSO technique introduced by Kennedy and Eberhart [7], with each particle memorizing its vector of position and velocity, as well as the time at which it reached its peak degree of fitness [8]. PSO starts with a random population and updates it to find optimal solutions. PSO has the advantage of requiring no evolution operators, such as mutation and crossover operators, and it does not necessitate the adjustment of many free parameters [9,10]. Farimah *et al.* [11] have discussed the optimization of the cumene process with statistical and genetic algorithm-based methods. Some researchers discuss artificial intelligence and machine learning approaches in chemical processes, especially the cumene production process [12–14].

In this work, authors have derived PID controllers [15] for studying the disturbance rejection and setpoint tracking of the cumene reactor, which is designed as a four-layer fixed bed catalytic reactor [16,17]. The major difficulty in the analysis is the availability of a system model for the process with high degrees of freedom [18,19]. The state space model of the system for the analysis is obtained from the COMSOL design of the system by MATLAB Livelink [20–22]. The classical PI and PID controllers based on Internal Model Control (IMC) are derived based on analytical rules [23,24]. P, PI, and PID controllers based on Zeigler Nichols tuning are developed as the system's basic controller for comparison [25]. PID controller based on Particle Swarm Optimisation is derived from studying the advantage of the evolutionary algorithm approach [26].

The major works included in the paper are: Derivation of system model for the plant (cumene reactor in HOCL, Kochi) from the state matrices obtained from COMSOL design [14]. Design of PI and PID controllers for the system using analytical rules and comparison. Design of IMC P, PI, and PID controller based on Zeigler Nichols tuning. PI controller design with particle swarm optimization and comparison with other controllers.

The paper is structured as follows. The first section details the cumene production process and state space model of the reactor. The second section

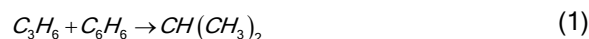
derives the PI and PID controllers design using analytical rules. P, PI, and PID controllers with Zeigler Nichols tuning are discussed in the following section. The following section explains the PI controller based on an evolutionary algorithm. The simulation results and comparative studies are also presented. The concluding comments are marked in the last section.

STATE MODEL OF THE CUMENE PROCESS

Cumene Production Process Description

The fundamental reaction in the cumene production process in the cumene plant is an alkylation process in which benzene and propylene react to form cumene in the presence of an acidic catalyst [20,27]. HOCL set up a cumene plant employing SPA catalyst in 1983 at Kochi. The used packed bed reactor has four layers of solid phosphoric acid beds [20,28].

The principal reaction is expressed as:



The simplified model of the reactor is given by Eqs. 2–4.

The mass balance equations are:

$$\begin{aligned} \epsilon_b \rho_g \frac{dw_B}{dt} &= \left(-\frac{M}{A_{int}} \frac{\partial w_B}{\partial z} + Mw_B(-r_B) \right) \dots (a) \\ \epsilon_b \rho_g \frac{dw_P}{dt} &= \left(-\frac{M}{A_{int}} \frac{\partial w_P}{\partial z} + Mw(-r_P) \right) \dots (b) \\ \epsilon_b \rho_g \frac{dw_C}{dt} &= \left(-\frac{M}{A_{int}} \frac{\partial w_C}{\partial z} + Mw_C r_C \right) \dots (c) \end{aligned} \quad (2)$$

where A_{int} is the inner cross-sectional area of the reactor, M is the mass flow rate, Mw_i is the molar weight of the i^{th} component, r_i is reaction rate of i^{th} species, ϵ_b is catalytic bed void fraction, ρ_g is gas phase density and w_B , w_P and w_C are the mass fractions of benzene, propylene, and cumene, respectively.

The reactor energy balance equation is:

$$\begin{aligned} (\epsilon_b \rho_g C_{pmix} + (1 - \epsilon_b) \rho_c C_{pcat}) \frac{dT}{dt} &= -\frac{M}{A_{int}} C_{pmix} \frac{\partial T}{\partial z} \\ &+ \pi \frac{U}{A_{int}} (T_{shell} - T) + r_c (-\Delta H_r) \end{aligned} \quad (3)$$

where ϵ_b is the catalytic bed void fraction, ρ_g is the gas phase density, C_{pmix} is the specific heat of the mixture, ρ_c is the catalytic pellet density, C_{pcat} is the specific heat of the catalyst, ρ_c is catalytic pellet density, A_{int} is the inner cross-sectional area of the reactor, M is the mass flow rate, U is the heat transfer coefficient, T_{shell} is the reactor shell side temperature and ΔH_r is the enthalpy of the reaction.

The rate of reaction is:

$$r_c = \rho_c (1 - \epsilon_b) \eta_1 r_1 \quad (4)$$

where

$$r_1 = k w_B w_C \text{ and } k = 3500 e^{\frac{13.28}{RT}} \quad (5)$$

ρ_c is catalytic pellet density, ϵ_b is catalytic bed void fraction, η_1 is reaction efficiency w_B and w_C are mass fractions of benzene and cumene, R is the universal gas constant, and T is the absolute temperature.

As a system with a large amount of uncertainty, it is very difficult to extract the state space model of the system. Besides, the system is represented by nonlinear partial differential equations, making the solution derivation more tedious. Incorporating the parameters from the studied plant, the system has been implemented in COMSOL Multiphysics to extract state transition matrices of the system [14].

Extraction of Model from COMSOL Multiphysics using Matlab Livelink

For many chemical processes, the state space modeling of the system is not available because of the high degrees of freedom. The COMSOL Multiphysics modeling of the reactor will help with the performance analysis and optimization of specific parameters [20]. A novel approach for extracting the state space matrices from COMSOL is utilized here. The state space matrices of the cumene production process have been obtained from the COMSOL design using MATLAB Livelink. The Continuous-time state-space model obtained has 11493 DOF. The system has been reduced to a 4th order system using model order reduction. The parameters used to simulate the model are listed in Table 1.

Table 1. Parameters used for simulation.

| Parameters | Unit for simulation |
|---|-------------------------|
| Height of the reactor | 15.3 m |
| Diameter of the reactor | 1.5 m |
| Diameter of the catalyst particle | 1 mm |
| Density of catalyst particle | 58000 kg/m ³ |
| Porosity of catalyst particle | 0.75 |
| Initial solid height | 150 mm |
| Bed porosity | 0.5 |
| Inlet feed velocity | 0.8 m/s |
| Inlet feed composition (C_6H_6, C_3H_8, C_3H_6) | 8:2:1 |
| Inlet feed temperature | 316 K |
| Inlet pressure | 32.9 atm |

The state space matrices obtained for the cumene production process after model order reduction are given in Eq. 6:

$$A = \begin{bmatrix} -0.5409 & 5.304 \times 10^{-7} & 1.52 \times 10^{-10} & 1.027 \times 10^{-6} \\ -1.939 \times 10^{-5} & -0.5077 & 1.96 \times 10^{-6} & -3.858 \times 10^{-10} \\ -0.00373 & -1.527 \times 10^{-5} & -0.4719 & 1.5 \times 10^{-5} \\ 1.021 \times 10^{-5} & 0.002405 & 1.947 \times 10^{-6} & -0.4492 \end{bmatrix} \quad (6)$$

$$B = \begin{bmatrix} 1.66 \times 10^{-17} \\ 1.286 \times 10^{-17} \\ 7.461 \times 10^{-17} \\ 1.31 \times 10^{-16} \end{bmatrix}$$

$$C = [1.878 \times 10^{-17} \quad 2.291 \times 10^{-17} \quad 9.192 \times 10^{-18} \quad 5.657 \times 10^{-18}]$$

$$D = [0]$$

INTERNAL MODEL CONTROL-BASED PI AND PID CONTROLLERS

The simple two-step procedure proposed by Sigurd Skogestad [1] has been adopted to design a controller for the cumene production process. The tuning rules should be well-motivated for a good controller, with a preference for model-based and analytically determined tuning rules. They should be simple to remember. They should be able to handle a wide range of tasks. The Internal Model Control PID, which satisfies the objectives of a good PID controller, provides the rules for system model reduction and design of the PID controller. Figure 1 shows the packed bed reactor structure and the system with feedback control. Here u is the manipulated input, d is the disturbance, y is the controlled output and y_s is the setpoint for controlled output. The process transfer function is represented by $(s) = \frac{\Delta y}{\Delta u}$, controller feedback is represented as $c(s)$. Δ , the deviation of the variables and s , the laplace variables are neglected to simplify the notation.

Using the proposed Skogestad half rule, the system's first and second-order plus delay model is derived. The controller settings can be derived based on the model. If we consider the first-order model plus delay model, it will result in PI controller settings, and if we start from the second-order plus delay model, PID controller settings can be obtained.

The PID settings are derived for the series form of PID controller as follows:

$$c(s) = K_c \left(\frac{\tau_1 + 1}{\tau_1 s} \right) (\tau_D s + 1) \quad (7)$$

$$c(s) = \frac{K_c}{\tau_1 s} (\tau_1 \tau_D s^2 + (\tau_1 + \tau_D) s + 1) \quad (8)$$

Step 1: Process model approximation

The model approximation includes the approxi-

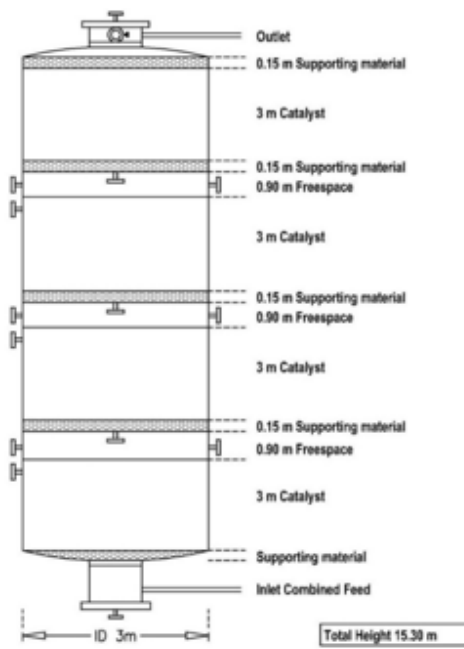


Figure 1. System with feedback control.

mation of the original model to a first- or second-order plus time delay model, $g(s)$. Skogestad half rules approximate first order plus dead time (FOPDT) and second order plus dead time (SOPDT) systems. For a system to apply Skogestad half rules, the denominator should be in terms of τs , and a dominant time constant should exist ($\tau_{largest} \geq 1.5\tau_{next\ largest}$) and the system should be stable. The parameters that need to be estimated for the model approximation are plant gain K , dominant lag time constant (τ in case FOPDT and τ_1 in case of SOPDT), time delay (dead time) θ , second-order lag time constant τ_2 ,

The approximate first order plus deadtime (FOPDT) model can be represented as

$$\frac{Ke^{-\theta s}}{\tau s + 1} \quad (9)$$

The parameters are obtained as follows:

$$K = K_{higher\ order}$$

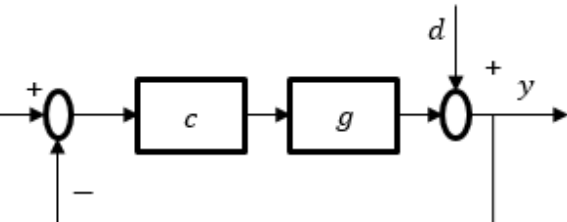
$$\tau = \tau_{largest} + 0.5\tau_{next\ largest}$$

$$\theta = 0.5\tau_{next\ largest} + \sum \tau + \theta_{higher\ order}$$

Approximated model after substituting the parameters is:

$$\frac{4.26 \times 10^{-33} e^{-10.942s}}{2.29s + 1} \quad (10)$$

Similarly, the approximate second-order plus deadtime model can be represented as:



$$\frac{Ke^{-\theta s}}{(\tau_1 s + 1)(\tau_2 s + 1)} \quad (11)$$

The parameters are obtained as:

$$K = K_{higher\ order}$$

$$\tau_1 = \tau_{largest}$$

$$\tau_2 = \tau_{next\ largest} + 0.5\tau_{second\ next\ largest}$$

$$\theta = 0.5\tau_{second\ next\ largest} + \sum \tau + \theta_{higher\ order}$$

Approximated model after substituting the parameters is:

$$\frac{4.26 \times 10^{-33} e^{-8.897s}}{(2.23s + 1)(3.105s + 1)} \quad (12)$$

Step 2: Internal model control based PID tuning

In this session, PI and PID controllers are derived for the FOPDT and SOPDT system using the direct synthesis method or the internal model control approach[1,3].

From the comparison of Eq. A9 and A10 (Supplementary materials), the parameters can be obtained as:

$$\tau_D = \tau_2; \tau_I = \tau_1; K_c = \frac{1}{K} \frac{\tau_1}{(\tau_c + \theta)} \quad (13)$$

The parameter values are obtained from the model, and the response is obtained for various tuning

values. The best tuning value is identified, and the integral terms are varied to obtain the best setpoint tracking and disturbance rejection.

P, PI, AND PID CONTROLLERS USING ZEIGLER NICHOLS TUNING

Ziegler-Nichols tuning is applied to the FOPDT model of the process to obtain the system's step response. The reaction curve process identification procedure is used to identify the parameters for P, PI, and PID settings. The inflection point is identified, and the tangent is plotted in the reaction curve. The values obtained are effective delay, D_e , process reaction rate, R_p and unit reaction rate, R_u ; these values are used for parameter setting. Parameter settings from the process reaction curve for P, PI, and PID controllers are given in Table 2.

Table 2. PID setting from process reaction curve.

| Type | K_c | T_i | T_d |
|------|---------------|-----------|----------|
| P | $1/R_u D_e$ | - | - |
| PI | $0.9R_u D_e$ | $3.33D_e$ | - |
| PID | $1.2/R_u D_e$ | $2D_e$ | $0.5D_e$ |

PSO PID CONTROLLER FOR THE SYSTEM

An evolutionary algorithm for PI tuning is introduced to compare the performance in settling time and rejection of disturbance with that of analytical rules. Particle swarm optimization algorithm, also known as bird swarm foraging algorithm, is used here for tuning the PI parameters, in which the idea originated from the study of the predation behavior of birds or fish. The particle swarm algorithm simulates so that the birds in the flock are considered massless particles. The attributes of each particle include position and velocity. Each particle searches for the optimal solution separately in the search space, determines the fitness value through the fitness function to evaluate the quality of the current position, and records the optimal solution. Particles are evolved by competition and corporation among themselves through generations. The particles adjust their speed and position according to the local and global optimal solutions. The analysis depicts the importance of computational techniques in controller design. The PSO algorithm to tune the PI parameter based on the best position and velocity is given in Figure 2.

PSO algorithm

The velocity of the particle:

$$g_{id}^k = w g_{id}^{k-1} + c_1 r_1 (pbest_{id} - x_{id}^{k-1}) + c_2 r_2 (gbest_{id} - x_{id}^{k-1}) \quad (14)$$

Position of the particle:

$$x_{id}^k = x_{id}^{k-1} + g_{id}^{k-1} \quad (15)$$

where,

v_{id} =velocity of the i^{th} particle

x_{id} =position of the i^{th} particle

k = discrete time constant

id = particle index

$pbest_{id}$ =best position found by the i^{th} particle

$gbest_{id}$ = best position found by the swarm

w = inertia factor

c_1, c_2 = acceleration constant

r_1, r_2 = random numbers [0,1]

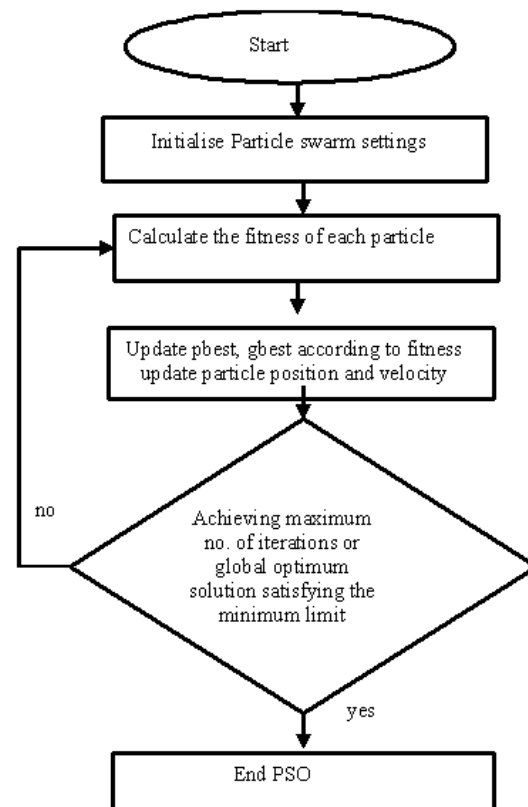


Figure 2. PSO algorithm.

SIMULATION RESULTS

IMC-based PI and PID controllers

The PI and PID controllers for the system with different tuning parameter values are designed. Figure 3 shows the PI controller with three different tuning parameters. $\tau_c=0$, $\tau_c=1$, and $\tau_c=1.5$. From the analysis, it can be identified that the PI and PID controllers with $\tau_c=1.5$ shows better disturbance rejection and setpoint tracking.

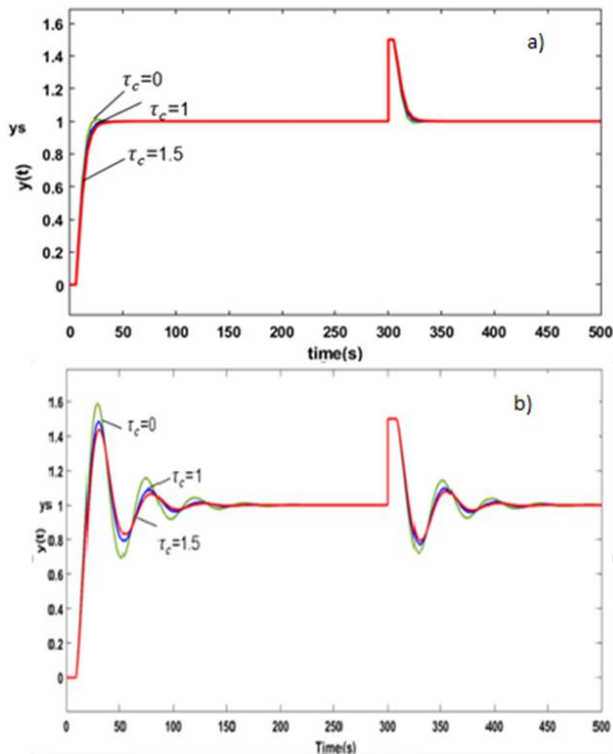


Figure 3. (a) PI and (b) PID controller with different tuning parameters.

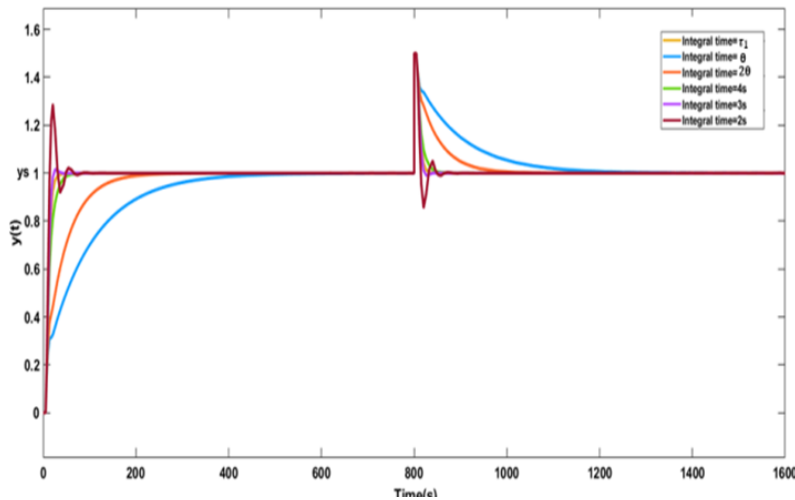


Figure 4. PI-control of the system with different integral times. $K_c = 9.63 \times 10^{33}$, change in setpoint is at $t = 0$ s and load disturbance is at $t = 800$ s.

To improve the disturbance rejection, the rule for an integral term is modified in the proposed IMC PI tuning. Figure 4 shows the effect of changing the integral time for PI-control of the system with $K_c = 9.63 \times 10^{33}$. The setpoint change is given at $t = 0$ s, and a load disturbance of 0.5 magnitude is applied at $t = 800$ s. The integral time has given the values as τ_{I1} , θ , 2θ , 4 s, 3 s, and 2 s.

Interpretation of PI controller output

$\tau_I = \tau_{I1} = 3.29$ s: excellent setpoint tracking and fast settling for a load disturbance.

$\tau_I = 2\theta$: setpoint response is poor and slow settling time for load disturbance.

$\tau_I = \theta$: even quicker settling and reaction to setpoints (and robustness).

$\tau_I = 4$ s: excellent setpoint tracking and faster settling time.

$\tau_I = 3$ s: good setpoint tracking and faster settling time.

$\tau_I = 2$ s: response is poor with slow settling time.

Table 3. Disturbance rejection and setpoint tracking for various values of integral time τ_I for PI controller.

| Type | Integral time | Unit setpoint change at $t=0$ s | | | | Load Perturbation of magnitude 10 at $t=800$ s | | | |
|-------------|----------------------|---------------------------------|-----------|-----------|-----------------|--|-----------|-----------|-----------------|
| | | t_p (s) | t_s (s) | M_p (%) | ϵ_{SS} | t_p (s) | t_s (s) | M_p (%) | ϵ_{SS} |
| Proposed PI | $\tau_I = \tau_{I1}$ | 0 | 45 | 0 | 0 | 0 | 38 | 0 | 0 |
| | $\tau_I = 2\theta$ | 0 | 600 | 0 | 0 | 0 | 520 | 0 | 0 |
| | $\tau_I = \theta$ | 0 | 350 | 0 | 0 | 0 | 60 | 0 | 0 |
| | $\tau_I = 4$ s | 0 | 75 | 0 | 0 | 0 | 60 | 0 | 0 |
| | $\tau_I = 3$ s | 25 | 45 | 1.5% | 0 | 30 | 40 | 2% | 0 |
| | $\tau_I = 2$ s | 21 | 110 | 28% | 0 | 20 | 100 | 14% | 0 |

A good trade-off between disturbance response and robustness is obtained by selecting the integral time. $\tau_I = \tau_1$, for the above system.

In the proposed IMC PID tuning, the rule for the integral term is modified to improve the disturbance rejection. Figure 5 shows the effect of changing the integral time for PID-control of the system with $K_c = 5.03 \times 10^{32}$. The setpoint change is given at $t=0$ s, and a load disturbance of 0.5 magnitude is applied at $t = 800$ s. The integral time has given the values as $\tau_1, \theta, 2\theta, 4, 3, 2$ s, and 2 s.

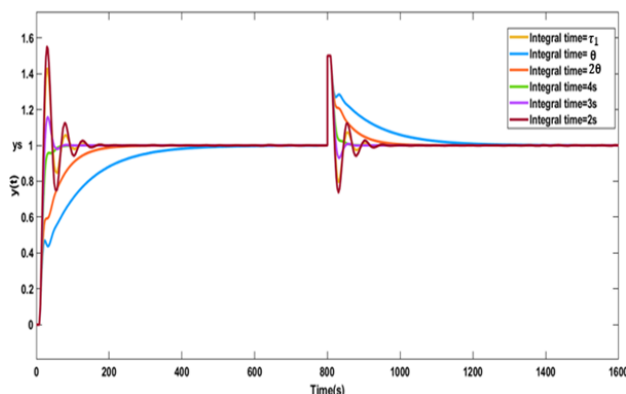


Figure 5. PID control of the system with different integral times. $K_c = 9.63 \times 10^{33}$, change in setpoint is at $t = 0$ s, and load disturbance is at $t = 800$ s.

Peak time t_p , settling time t_s , peak overshoot M_p , and steady-state error ϵ_{ss} corresponding to the disturbance rejection and setpoint tracking for the PID controller are shown in Table 4.

Interpretation of PID controller output

$\tau_I = \tau_1 = 2.203$ s: poor response with slow oscillations.

$\tau_I = 2\theta$: slow setpoint response and slow settling.

$\tau_I = \theta$: even faster settling and setpoint response (and robustness).

$\tau_I = 4$ s: excellent setpoint tracking and faster settling time.

$\tau_I = 3$ s: slow oscillations in setpoint tracking and faster settling time.

$\tau_I = 2$ s: poor response with oscillations.

A good trade-off between disturbance response and robustness is obtained by selecting the integral time. $\tau_I = 4$ s, which corresponds to the above system.

Table 4. Disturbance rejection and setpoint tracking for various values of integral time, τ_I for PID controller.

| Integral Types time | Unit setpoint change at $t=0$ s | | | | Load Perturbation of magnitude 10 at $t=800$ s | | | | |
|---------------------|---------------------------------|-----------|-----------|-----------------|--|-----------|-----------|-----------------|---|
| | t_p (s) | t_s (s) | M_p (%) | ϵ_{ss} | t_p (s) | t_s (s) | M_p (%) | ϵ_{ss} | |
| Proposed PID | $\tau_I = \tau_1$ | 29 | 160 | 43% | 0 | 30 | 150 | 20% | 0 |
| | $\tau_I = 2\theta$ | 0 | 570 | 0 | 0 | 0 | 600 | 0 | 0 |
| | $\tau_I = \theta$ | 0 | 300 | 0 | 0 | 0 | 350 | 0 | 0 |
| | $\tau_I = 4$ s | 0 | 103 | 0 | 0 | 0 | 95 | 0 | 0 |
| | $\tau_I = 3$ s | 32 | 100 | 16% | 0 | 30 | 70 | 7% | 0 |
| | $\tau_I = 2$ s | 29 | 500 | 57% | 0 | 30 | 200 | 26% | 0 |

Comparison of IMC-based PI and PID controllers

The comparison of PI and PID controllers has been done for various values of integral time. Figure 6 shows that the PI controller has a better-set point tracking disturbance rejection than the PID controller. Table 5 gives the comparison of PI and PID controllers for $\tau_I = \tau_1$ and $\tau_I = 4$ s. The controllers corresponding to these values have better setpoint tracking and disturbance rejection than other integral values. In the PI controller, $\tau_I = \tau_1$ gives a better response, where $\tau_I = 4$ s gives a better setpoint tracking disturbance rejection, as in the case of the PID controller.

P, PI, and PID controllers with Zeigler Nichols Tuning

This analysis uses the parameter obtained from the process reaction curve for parameter setting. For

the controller setting, the unit reaction rate, R_u and effective delay, D_e obtained from the reaction curve are used for calculating K_c , T_i , and T_d . The parameter values obtained for P, PI, and PID controllers are given in Table 6.

A comparative study of P, PI, and PID controllers derived from Zeigler Nichols's PID setting is done in this section. The response of P, PI, and PID controllers for a setpoint change given at $t = 0$ s, and a load disturbance of magnitude 0.5 applied at $t = 800$ s is given in Figure 7. It can be identified that the PI controller gives better setpoint tracking compared to the sluggish nature of the PID controller. The analysis of both IMC and Zeigler Nichols controllers depicts that the PI controllers best suit the cumene production process with improved robustness and stability.

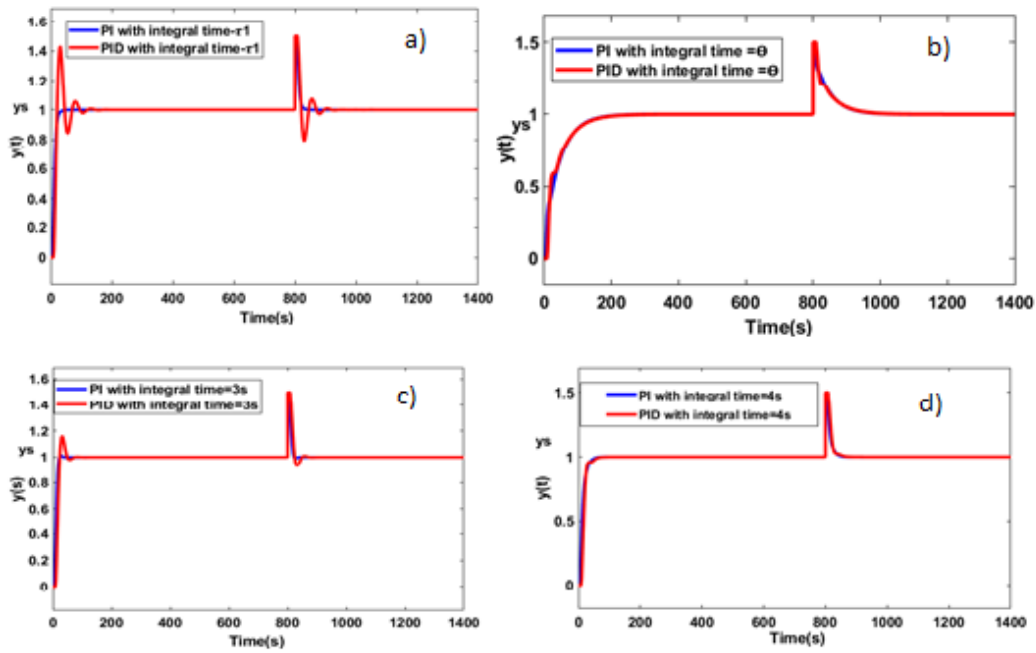


Figure 6. Comparison of PI and PID controllers done for various values of integral times, τ_i (a) $\tau_i = \tau_1$, (b) $\tau_i = 0$, (c) $\tau_i = 3\text{ s}$, and (d) $\tau_i = 4\text{ s}$.

Table 5. Disturbance rejection and setpoint tracking for PI and PID controllers.

| Integral Types time | Unit Setpoint change at t=0 s | | | | Load Perturbation of magnitude 10 at t=800 s | | | |
|---------------------|-------------------------------|-----------|-----------|-----------------|--|-----------|-----------|-----------------|
| | t_p (s) | t_s (s) | M_p (%) | ϵ_{ss} | t_p (s) | t_s (s) | M_p (%) | ϵ_{ss} |
| Proposed PI | $\tau_i = \tau_1$ | 35 | 45 | 0 | 0 | 38 | 0 | 0 |
| | $\tau_i = 4\text{ s}$ | 0 | 75 | 0 | 0 | 60 | 0 | 0 |
| Proposed PID | $\tau_i = \tau_1$ | 29 | 160 | 43% | 0 | 30 | 20% | 0 |
| | $\tau_i = 4\text{ s}$ | 0 | 103 | 0 | 0 | 95 | 0 | 0 |

Table 6. Zeigler Nichols PID setting.

| Type | K_c | T_i (s) | T_d (s) |
|------|-------------------------|-----------|-----------|
| P | 7.538×10^{31} | - | - |
| PI | 6.784×10^{31} | 36.437 | - |
| PID | 9.0456×10^{31} | 21.884 | 5.4710 |

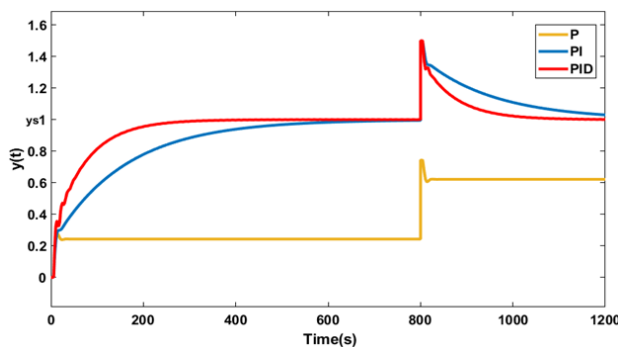


Figure 7. P, PI, and PID controller response with Zeigler Nichols tuning.

PI controller with PSO

The IMC and ZN-based controller simulation results emphasize that the PI controller is the apt controller for this production process. In this part, the PI

controller tuning is obtained with particle swarm optimization algorithm. 50 iterations are considered for a population size of 50. The Inertia weight is taken as 0.9. Other parameters used for optimization are given in Table 7.

Table 7. Variables in PSO.

| Variables | Values |
|---------------------------|--------|
| Dimension | 2 |
| Population | 50 |
| Iterations | 50 |
| Cognitive coefficient, c1 | 0.12 |
| Social coefficient, c2 | 1.2 |
| Inertia weight | 0.9 |

Comparative study of PSO PI controller with and Zeigler Nichols tuning PI controller

PSO PI controller based on evolutionary algorithm gives excellent response for setpoints without any oscillations, and settling time is very small for a load disturbance compared to Zeigler Nichols and IMC PI controllers. A comparison of IMC-PI, PSO, and ZN PI controllers for setpoint tracking and disturbance

rejection comparison is shown in Figure 8. The analysis in Table 8 tells that the PSO PI controller settles at 45 s without any oscillations and settles down faster for the disturbance of magnitude 0.5 applied at $t = 800$ s.

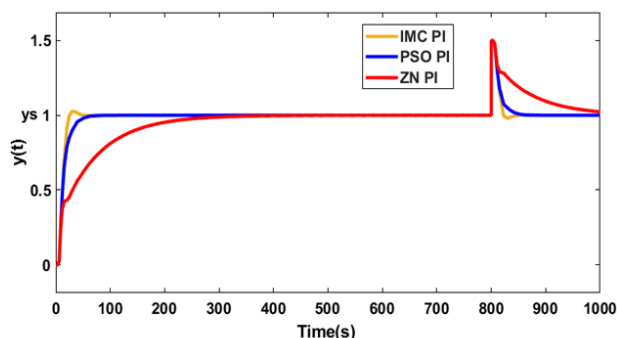


Figure 8. Setpoint tracking and disturbance rejection comparison of the PSO PI controller and comparison with the IMC and ZN PI controllers.

Table 8. Setpoint tracking and disturbance rejection comparison.

| Controller Types | Unit setpoint change at $t = 0$ s | | | | Load perturbation of magnitude 10 at $t = 800$ s | | | |
|------------------|-----------------------------------|-------|-------|-----------------|--|-------|-------|-----------------|
| | t_p | t_s | M_p | ϵ_{ss} | t_p | t_s | M_p | ϵ_{ss} |
| | (s) | (s) | (%) | | (s) | (s) | (%) | |
| IMC PI | 30 | 45 | 0 | 0 | 0 | 38 | 0 | 0 |
| ZN PI | 0 | 300 | 0 | 0 | 0 | 200 | 0 | 0 |
| PSO PI | 0 | 45 | 0 | 0 | 0 | 38 | 0 | 0 |

The comparative study of different classical control strategies shows that the PSO PI controller exhibits excellent setpoint tracking and disturbance rejection compared to other modeling strategies. Besides that, compared to the PID controller, the PI controller suites better for this particular process.

CONCLUSION

A comparative study of different classical control strategies was done for the cumene production process as a part of modeling and control of the process. As a system with a large amount of uncertainty, the state space matrices of the cumene production process were obtained from the COMSOL design using MATLAB Livelink. The IMC-based PI and PID controllers are derived for the performance analysis, and the controller with analytical rules is compared with that of Zeigler Nichols tuning and Particle swarm optimization. The single-tuning parameter τ_c is adjusted in the PI and PID controller with the analytical rules for the optimum response. The integral terms can be further adjusted for improved disturbance rejection and setpoint tracking.

The P, PI, and PID controllers of Zeigler Nichols tuning are designed with process curve approximations and it is found that the PI controller has the best approximation. The evolutionary computation technique is used for the PID controller setting to check the improvement in response. Particle swarm optimization is used for the PID tuning, and it is observed that the PI controller with PSO shows better disturbance rejection and setpoint tracking with a minimum settling time.

ACKNOWLEDGMENT

The authors thank the team HOCL, Kochi, Kerala, for their timely support in completing the work. They would like to thank all the anonymous referees for their suggestions for improving this paper.

ABBREVIATIONS

| | |
|-------|-----------------------------|
| FOPDT | First Order Plus Dead Time |
| SOPDT | Second Order Plus Dead Time |
| IMC | Internal Model Control |
| PSO | Particle Swarm Optimization |

REFERENCES

- [1] S. Skogestad, J. Process Control. 13 (2003) 291–309. [https://doi.org/10.1016/S0959-1524\(02\)00062-8](https://doi.org/10.1016/S0959-1524(02)00062-8).
- [2] J.G. Ziegler, N.B. Nichols, Trans. ASME. 64 (1942) 759–765. <https://doi.org/10.1115/1.4019264>.
- [3] D.E. Rivera, M. Morari, S. Skogestad, Ind. Eng. Chem. Process Des. Dev. 25 (1986) 252–265. <https://doi.org/10.1021/i200032a041>.
- [4] B.D. Tyreus, W.L. Luyben, Ind. Eng. Chem. Res. 31 (1992) 2625–2628. <https://doi.org/10.1021/ie00011a029>.
- [5] K.J. Astrom, P.I.D. Controllers, Theory, Design, and Tuning, Instrument Society of America, Research Triangle Park, North Carolina (1995).
- [6] K.J. Astrom, T. Hägglund, J. Process Control. 14 (2004) 635–650. <https://doi.org/10.1016/j.jprocont.2004.01.002>.
- [7] R. Eberhart, J. Kennedy, Particle Swarm Optimization, in Proceedings of the IEEE International Conference on Neural Networks, Citeseer, (1995) 1942–1948.
- [8] W. Zeng, W. Zhu, T. Hui, L. Chen, J. Xie, T. Yu, Nucl. Eng. Des. 360 (2020) 110513. <https://doi.org/10.1016/j.nucengdes.2020.110513>.
- [9] F. Marini, B. Walczak, Chemom. Intell. Lab. Syst. 149 (2015) 153–165. <https://doi.org/10.1016/j.chemolab.2015.08.020>.
- [10] D. Wang, D. Tan, L. Liu, Soft Comput. 22 (2018) 387–408. <https://doi.org/10.1007/s00500-016-2474-6>.
- [11] F. Mahmoudian, A.H. Moghaddam, S.M. Davachi, Can. J. Chem. Eng. 100 (2022). 90–102.

- <https://doi.org/10.1002/cjce.24072>.
- [12] A.H. Moghaddam, J. Shayegan, J. Sargolzaei, J. Taiwan Inst. Chem. Eng. 62 (2016) 150–157. <https://doi.org/10.1016/j.jtice.2016.01.024>.
- [13] A. HedayatiMoghaddam, H. Hazrati, J. Sargolzaei, J. Shayegan, A, Appl. Water Sci. 7 (2017) 2753–2765. doi:10.1007/s13201-016-0503-3.
- [14] H. Vaziri, A. HedayatiMoghaddam, S.A. Mirmohammadi, Chem. Pap. 74 (2020) 3311–3324. doi:10.1007/s11696-020-01162-w.
- [15] S. Bennett, Annu. Rev. Control 25 (2001) 43–53. [https://doi.org/10.1016/S1367-5788\(01\)00005-0](https://doi.org/10.1016/S1367-5788(01)00005-0).
- [16] V.M. Lakshmanan, A. Kallingal, S. Sreekumar, J. Indian Chem. Soc. 99 (2022) 100730. <https://doi.org/10.1016/j.jics.2022.100730>.
- [17] V.M. Lakshmanan, A. Kallingal, S. Sreekumar, J. Control Decis. (2022) 1–11. <https://doi.org/10.1080/23307706.2022.2146009>
- [18] V. Gera, M. Panahi, S. Skogestad, N. Kaistha, Ind. Eng. Chem. Res. 52 (2013) 830–846. <https://doi.org/10.1021/ie301386h>.
- [19] A. Chudinova, A. Salischeva, E. Ivashkina, O. Moizes, A. Gavrikov, Procedia Chem. 15 (2015) 326–334. <https://doi.org/10.1016/j.proche.2015.10.052>.
- [20] V.M. Lakshmanan, A. Kallingal, S. Sreekumar, Int. J. Chem. React. Eng. (2021) 1–17. <https://doi.org/10.1080/23307706.2022.2146009>.
- [21] X. Yang, S. Wang, B. Li, Y. He, H. Liu, Fuel 274 (2020) 117829. <https://doi.org/10.1016/j.fuel.2020.117829>.
- [22] H.M. Park, Int. J. Heat Mass Transfer 116 (2018) 520–531. <https://doi.org/10.1016/j.ijheatmasstransfer.2017.09.035>.
- [23] U.M. Nath, C. Dey, R.K. Mudi, IETE J. Res. (2021) 1–21. <https://doi.org/10.1080/03772063.2021.1874839>.
- [24] S.K. Pradhan, D. Acharya, D.K. Das, Ann. Nucl. Energy 165 (2022) 108675. <https://doi.org/10.1016/j.anucene.2021.108675>.
- [25] Z. Nie, Z. Li, Q. Wang, Z. Gao, J. Luo, Int. J. Robust Nonlinear Control. (2021). <https://doi.org/10.1002/rnc.5848>.
- [26] S. Sreekumar, A. Kallingal, L.V. Mundakkal, Chem. Ind. Chem. Eng. Q. 28(2) (2022) 127–134. <https://doi.org/10.2298/CICEQ200911031S>.
- [27] P.G. Junqueira, P.V. Mangili, R.O. Santos, L.S. Santos, D.M. Prata, Chem. Eng. Process. 130 (2018) 309–325. <https://doi.org/10.1016/j.cep.2018.06.010>.
- [28] M.L. Vinila, K. Aparna, S. Sreepriya, in Int. Conf. Intell. Comput. Inf. Control Syst., Springer, 2019: pp. 201–208. https://doi.org/10.1007/978-3-030-30465-2_23.

VINILA MUNDAKKAL
LAKSHMANAN^{1,2}
APARNA KALLINGAL¹
SREEPRIYA SREEKUMAR^{1,2}

¹Department of Chemical
Engineering, National Institute of
Technology Calicut, Kozhikode,
Kerala, India

²Department of Robotics and
Automation, Adi Shankara
Institute of Engineering and
Technology, Kalady, India

UNUTRAŠNJI MODEL KONTROLE KUMENSKOG PROCESA KORIŠĆENJEM ANALITIČKIH PRAVILA I EVOLUCIONOG RAČUNARSTVA

Kumen (izopropilbenzen) je prekursor za proizvodnju mnogih organskih hemikalija i razređivača za boje i lakove. Njegov proizvodni proces uključuje složenu kinetiku. Različite klasične strategije upravljanja za kumenski reaktor su implementirane i upoređene u ovom procesu. Za ovakav sistem sa velikim stepenom slobode, usvojen je novi pristup za izdvajanje modela u prostora stanja iz programskog paketa COMSOL Multiphysics. Za sistem su izvedeni PI i PID kontroleri zasnovani na internoj modernoj kontroli (IMC). Da bi se izvelo podešavanje kontrolera korišćenjem Skogestad polupravila, sistem je sveden na strukturu modela FOPDT i SOPDT. Integralno vreme je modifikovano za praćenje zadate tačke i brže odbacivanje smetnji. Iz analize se može konstatovati da PI kontroler više odgovara ovom specifičnom procesu. Algoritam za optimizaciju roja čestica (PSO), evoluciona tehnika izračunavanja, takođe se koristi za podešavanje PI podešavanja. Upoređeni su PI kontroleri sa podešavanjem IMC, Zeigler Nichols i PSO i može se zaključiti da se PSO PI kontroler smiruje za 45 s bez ikakvih oscilacija i brže se slaže za poremećaj veličine 0,5 primenjen na t = 800 s. Međutim, on je računarski intenzivan u poređenju sa drugim strategijama kontrolera.

Ključne reči: IMC PI, IMC PID, Skogestad polupravilo, Zeigler Nichols, PSO PI.